



<b>Beamline:</b> ID08	<b>Experiment title:</b> <b>Element-Resolved Ferromagnetic Resonance of Metal Multilayers</b>	<b>Experiment number:</b> HE 2087
<b>Shifts:</b> 18	<b>Date of experiment:</b> from: 12/06/2006 to: 20/06/2006  <b>Local contact(s):</b> Dr. P. Bencok	<b>Date of report:</b> 31/08/2006  <i>Received at ESRF:</i>
<b>Names and affiliations of applicants:</b> P. Gambardella <sup>¶</sup> , S. Stepanow <sup>¶</sup> , S. Rusponi <sup>*</sup> , G. Boero <sup>*</sup> , P. Bencok <sup>#</sup> <sup>¶</sup> <i>Catalan Institute of Nanotechnology, Universitat Autònoma de Barcelona, 08193 Spain</i> <sup>*</sup> <i>Ecole Polytechnique Fédérale de Lausanne, CH-1015 Lausanne</i> <sup>#</sup> <i>ESRF, BP 220, F-38043 Grenoble</i>		

The proposed experiment aimed at resolving elemental ferromagnetic resonance (FMR) spectra in heterogeneous metal systems using an XMCD-based technique recently developed by our groups at the ESRF [1]. Rather than using time-resolved pump-probe XMCD measurements as is currently done in a number of experiments at the ESRF, SLS, ALS, and APS [see, e.g., 2-4] we rely on a complementary approach in the frequency domain, namely the measurement of continuous-wave FMR spectra by time-averaged XMCD in magnetic samples resonantly excited at microwave (MW) frequencies. The experimental setup is shown in Fig. 1 and further explained in Ref. 1. The method exploits the XMCD dependence on the relative orientation between the sample magnetization  $\mathbf{M}$  and photon polarization  $\mathbf{P}$  to detect changes in the x-ray absorption signal due to the resonant excitation of precessional modes that reduce the projection of  $\mathbf{M}$  about the equilibrium direction  $z$ , which is set parallel to  $\mathbf{P}$  by an external field  $\mathbf{B}_0$ . Experiment HE 2087 was carried out at the ID08 beamline using the circularly polarized photon beam generated by two helical undulators operated in series. The beam incidence direction was aligned with  $\mathbf{B}_0$  and set perpendicular to the sample surface. X-ray absorption spectra (XAS) were measured by recording the sample fluorescence yield by means of a Si photodiode as a function of the incident photon energy (DC mode). X-ray FMR spectra (XFMR) were recorded as a function of  $B_0$  by lock-in detection of the photodiode current at fixed photon energy in the presence of a pulse-modulated microwave field (AC mode). The XMFR data presented here represent the difference of two consecutively recorded AC spectra for opposite photon polarization, analogously to the DC XMCD signal.

A number of remarkable results were obtained during the beamtime. I. We demonstrated for the first time the measurement of element-resolved FMR spectra. II. We showed that, in agreement with Kittel's theory, the so-called "ferromagnetic resonance mode" of a ferrimagnet is composed by the precession of two antiparallel moments that are rigidly coupled together. III. XFMR measurements can be extended to metal films less than 1 nm thick, providing element-specific FMR spectra of multilayer systems and information on interlayer coupling strength. IV. We showed that information on the dynamics of the spin vs. orbital magnetic moment can be obtained.

To prove I and II we used a 30  $\mu\text{m}$ -thick Gd-doped Yttrium Iron Garnet (YIG) polycrystalline sample. In this system, the magnetization of the Gd sublattice is antiferromagnetically coupled with respect to the Fe sublattice, producing a resultant magnetization  $4\pi M_s = 0.10$  T at room temperature, parallel to the Fe moment. The inductive FMR and XFMR spectra of Gd:YIG are shown in Fig. 2. We first remark that, although the resonance field  $B_{\text{res}}$  for the spectra in (a) and (b) is close to the expected Kittel's value

$B_{\text{res}} = \omega/\gamma + 4\pi M_s = 0.18$  T, the XFMR peak is shifted and much narrower compared to the FMR resonance. The latter, which shows clear signs of saturation due to the high level of MW power, is very likely broadened by the effects of inhomogeneous demagnetizing fields that vary across the sample dimensions. The XFMR signal, on the other hand, has a FWHM linewidth of less than 15 mT, in agreement with that of polished polycrystalline Gd:YIG spheres. We ascribe this effect to the inherent surface sensitivity of XFMR, which probes only a thin slice of the sample with dimensions much smaller compared to the spatial variation of the magnetostatic field. Fe and Gd XFMR spectra have been recorded with photon energies corresponding to the maxima of the DC XMCD at the Fe  $L_2$  edge (723 eV) and Gd  $M_4$  edge (1222 eV). The reversed sign of the Gd XFMR with respect to Fe is a signature of the antiferromagnetic dynamic coupling of the two sublattices. Moreover, the resonant field and the linewidth of the Gd and Fe peaks coincide within the experimental resolution (2 G), indicating that the Gd and Fe precessing moments are rigidly coupled and have common damping mechanisms.

Results III and IV were obtained for a NiFe/Ni polycrystalline bilayer with the following structure: 10 nm Al/ 5 nm Fe<sub>20</sub>Ni<sub>80</sub>/ 50 nm Ni/ 5 nm Cr /glass. Figure 3 shows the inductive (a) and XFMR (b) spectra of this sample. The Ni and Fe XFMR allowed us to clearly identify the lower resonance as that of the 50 nm Ni layer, and the higher one as that of the 5 nm NiFe layer, where the elemental Ni and Fe magnetization precess in phase [3], yielding two nearly identical XFMR peaks. The two resonances at 0.53 and 0.74 T are significantly lowered compared to those measured for single Ni and NiFe layers (0.6 and 1 T, respectively) owing to the ferromagnetic exchange coupling occurring at the NiFe/Ni interface [5]. Our results show that the two precessional modes are not mixed in this case, contrary to thinner bilayer structures where coupled optical and acoustical modes are observed [6]. Recording the XFMR signal at fixed field  $B_{\text{res}}$  as a function of photon energy allowed us to compare the dynamic XMCD spectrum with the static XMCD recorded in the DC mode with no MW field applied (Fig. 4). The relative spectral weight in the  $L_3$  vs.  $L_2$  edges appears to be similar, within the noise level of the experiment, indicating that the orbital magnetization follows the spin precessional motion. Longer data acquisition times are however required to settle this point unambiguously.

Finally, we wish to comment on the sensitivity of the present measurements. The Fe content in 5 nm permalloy corresponds to a 1 nm thick Fe layer equivalent. We believe that there are no obstacles to go beyond this limit, although it is hard to place a sensitivity boundary at this stage. Notably, the intensity of the XFMR peak of Ni (Fe) in Fig.3 corresponds to only 0.05% of the total Ni (Fe) XMCD for the same applied field, which represents a remarkable detection capability for a soft x-ray dichroism experiment.

The results presented in this report are still in the course of analysis and will be the object of a future publication [7].

## References

- [1] G. Boero, S. Rusponi, P. Bencok, H. Brune, R.S. Popovic, and P. Gambardella, *Appl. Phys. Lett.* **87**, 152503 (2005).
- [2] M. Bonfim et al., *Phys. Rev. Lett.* **86**, 3646 (2001).
- [3] W.E. Bailey, L. Cheng, D.J. Keavney, C.C. Kao, E. Vescovo, and D.A. Arena, *Phys. Rev. B* **70**, 172403 (2004).
- [4] S.-B. Choe et al., *Science* **304**, 420 (2004).
- [5] J.F. Cochran, B. Heinrich, and A.S. Arrott, *Phys. Rev. B* **34**, 7788 (1986).
- [6] B. Heinrich and J.F. Cochran, *Adv. Phys.* **42**, 523 (1993); M. Farle, *Rep. Prog. Phys.* **61**, 755 (1998)
- [7] G. Boero, S. Rusponi, P. Bencok, F. Nolting, S. Stepanow, and P. Gambardella, in preparation.

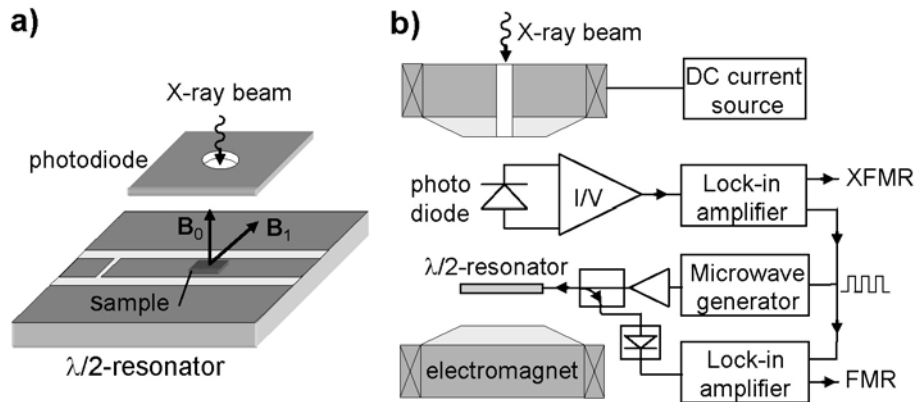


Fig 1. (a) Diagram of the sample, resonator, and fluorescence yield photodiode setup. (b) Overview of the experimental setup.

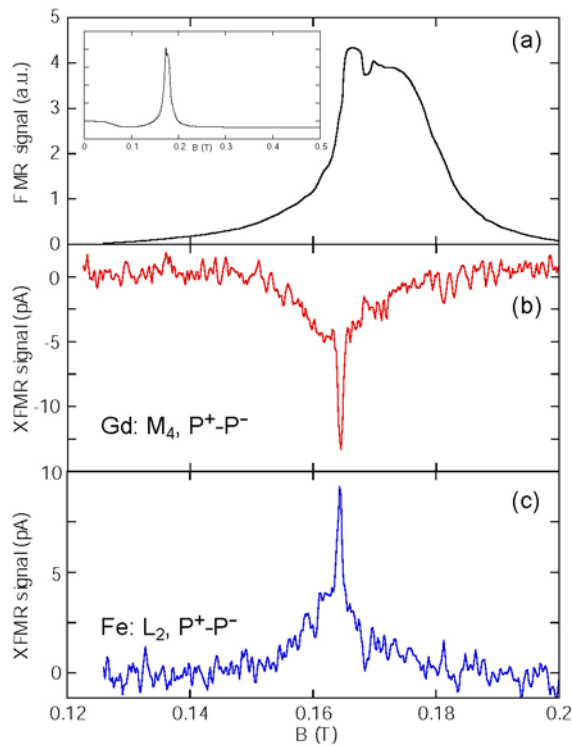


Fig. 2 (a) Inductive FMR spectrum of Gd:YIG near MW saturation conditions. Inset: extended-range of the FMR signal. (b) Gd XFMR spectrum recorded at the  $M_4$  Gd edge simultaneously with the FMR in (a). (c) Fe XFMR spectrum recorded at the  $L_2$  Fe edge. MW power = 1.25 W ( $B_1 \approx 0.35$  mT), MW frequency = 2.2 GHz.

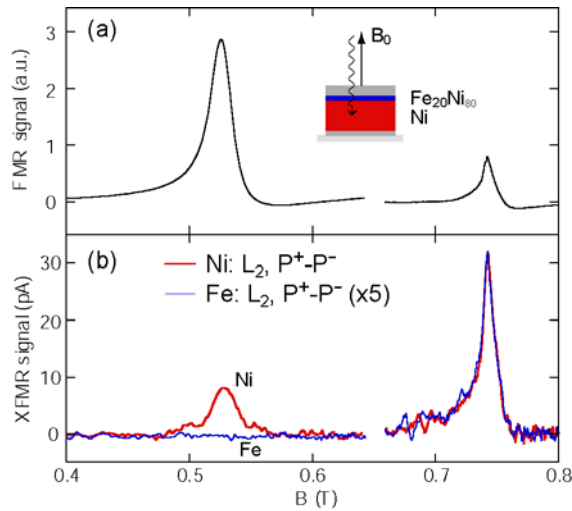


Fig. 3 (Top) Inductive FMR spectrum of a 5 nm  $\text{Fe}_{20}\text{Ni}_{80}$ / 50 nm Ni bilayer. (Bottom) Corresponding element-resolved XFMR spectra at the  $L_2$  Ni and Fe edges. MW power = 2.5 W ( $B_1 \approx 0.5$  mT), MW frequency = 2.14 GHz.

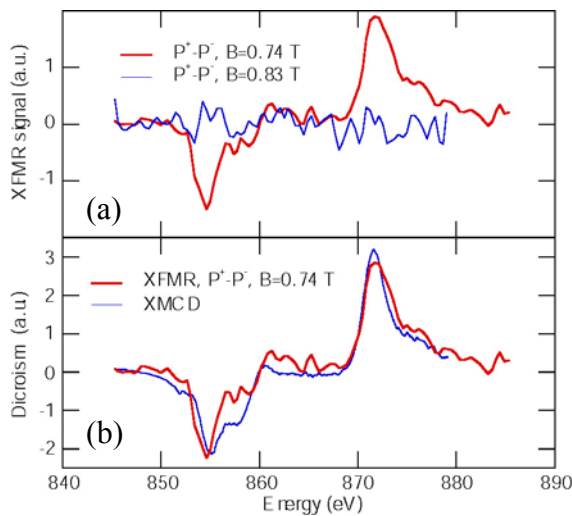


Fig. 4 (a) Ni XFMR signal vs. photon energy spectrum recorded at the resonant field (0.74 T, red solid line) and off-resonance (0.83 T, blue solid line) in NiFe. (b) Comparison of Ni XFMR and XMCD energy spectra. The spectra have been rescaled by an arbitrary constant factor for comparison. MW power  $\approx 2.5$  W ( $B_1 \approx 0.5$  mT), MW frequency  $\approx 2.2$  GHz.